



<i>Title:</i> NEON Algorithm Theoretical Basis Document (ATBD): TIS Soil Heat Flux		<i>Date:</i> 02/05/2020
<i>NEON Doc. #:</i> NEON.DOC.000814	<i>Author:</i> N. Pingintha-Durden	<i>Revision:</i> B

## ALGORITHM THEORETICAL BASIS DOCUMENT (ATBD):

### TIS SOIL HEAT FLUX

<b>PREPARED BY</b>	<b>ORGANIZATION</b>	<b>DATE</b>
Natchaya Pingintha-Durden	FIU	05/18/2016
Josh Roberti	FIU	05/18/2015
Hank Loescher	FIU	10/06/2012
Edward Ayres	FIU	01/17/2020

<b>APPROVALS</b>	<b>ORGANIZATION</b>	<b>APPROVAL DATE</b>
Kate Thibault	SCI	01/31/2020

<b>RELEASED BY</b>	<b>ORGANIZATION</b>	<b>RELEASE DATE</b>
Anne Balsley	CM	02/05/2020

See configuration management system for approval history.

The National Ecological Observatory Network is a project solely funded by the National Science Foundation and managed under cooperative agreement by Battelle. Any opinions, findings, and conclusions or recommendations expressed in this material are those of the author(s) and do not necessarily reflect the views of the National Science Foundation.



<i>Title:</i> NEON Algorithm Theoretical Basis Document (ATBD): TIS Soil Heat Flux		<i>Date:</i> 02/05/2020
<i>NEON Doc. #:</i> NEON.DOC.000814	<i>Author:</i> N. Pingintha-Durden	<i>Revision:</i> B

## Change Record

<b>REVISION</b>	<b>DATE</b>	<b>ECO #</b>	<b>DESCRIPTION OF CHANGE</b>
A	07/06/2016	ECO-03910	Initial Release
B	02/05/2020	ECO-06373	Removed references to specific installation depths, calibration frequencies, and calibration durations, and noted that these are subject to change. Other minor text edits.



Title: NEON Algorithm Theoretical Basis Document (ATBD): TIS Soil Heat Flux		Date: 02/05/2020
NEON Doc. #: NEON.DOC.000814	Author: N. Pingintha-Durden	Revision: B

**TABLE OF CONTENTS**

**1 DESCRIPTION.....1**

1.1 Purpose ..... 1

1.2 Scope..... 1

**2 RELATED DOCUMENTS, ACRONYMS AND VARIABLE NOMENCLATURE .....2**

2.1 Applicable Documents ..... 2

2.2 Reference Documents..... 2

2.3 Acronyms ..... 2

2.4 Variable Nomenclature ..... 3

**3 DATA PRODUCT DESCRIPTION.....4**

3.1 Variables Reported ..... 4

3.2 Input Dependencies ..... 4

3.3 Product Instances..... 4

3.4 Temporal Resolution and Extent ..... 4

3.5 Spatial Resolution and Extent ..... 5

**4 SCIENTIFIC CONTEXT .....5**

4.1 Theory of Measurement ..... 5

4.2 Theory of Algorithm ..... 6

4.2.1 Time regularization ..... 9

**5 ALGORITHM IMPLEMENTATION.....9**

**6 UNCERTAINTY .....13**

6.1 Uncertainty of Soil Heat Flux Measurements ..... 13

6.1.1 Measurement Uncertainty..... 14

6.1.2 Uncertainty of L1 Mean Data Product ..... 19

6.2 Uncertainty Budget..... 23

**7 FUTURE PLANS AND MODIFICATIONS.....25**

**8 BIBLIOGRAPHY .....26**

**LIST OF TABLES AND FIGURES**

Table 3-1: List of soil heat flux related L0 DPs that are transformed into L1 DPs in this ATBD. .... 4



<i>Title:</i> NEON Algorithm Theoretical Basis Document (ATBD): TIS Soil Heat Flux		<i>Date:</i> 02/05/2020
<i>NEON Doc. #:</i> NEON.DOC.000814	<i>Author:</i> N. Pingintha-Durden	<i>Revision:</i> B

Table 5-1: Flags associated with soil heat flux measurements..... 12

Table 5-2: Information maintained in the CI data store for with soil heat flux measurements..... 12

Table 6-1: Uncertainty budget for individual soil heat flux measurements. Shaded rows denote the order of uncertainty propagation (from lightest to darkest)..... 23

Table 6-2: Uncertainty budget for L1 mean soil heat flux DPs. Shaded rows denote the order of uncertainty propagation (from lightest to darkest)..... 24

Figure 1. Conceptual schematic of a heat flux sensor (source: RD [04]). ..... 5

Figure 2. A conceptual plot of the voltage output ( $V_s$ ) from the sensor when performing a self-calibration. .... 7

Figure 3. (a) Diagram of the position of the HFP01SC sensors within the soil array and (b) consistency test flow diagram for the HFP01SC sensor deployed at position 2. .... 26



<i>Title:</i> NEON Algorithm Theoretical Basis Document (ATBD): TIS Soil Heat Flux		<i>Date:</i> 02/05/2020
<i>NEON Doc. #:</i> NEON.DOC.000814	<i>Author:</i> N. Pingintha-Durden	<i>Revision:</i> B

## 1 DESCRIPTION

Contained in this document are details concerning soil heat flux measurements made at all NEON sites. Specifically, the processes necessary to convert “raw” sensor measurements into meaningful scientific units and their associated uncertainties are described.

### 1.1 Purpose

This document details the algorithms used for creating NEON Level 1 (L1) data products (DP) from Level 0 data, and ancillary data as defined in this document (such as calibration data), obtained via instrumental measurements made by Hukseflux HFP01SC: Self-Calibrating Heat Flux Sensor™ [NEON P/N: 0300260000]. It includes a detailed discussion of measurement theory and implementation, theoretical background, data product provenance, quality assurance and control methods used, assumptions, and a detailed estimation of uncertainty resulting in a cumulative uncertainty budget for this product.

### 1.2 Scope

The theoretical background and entire algorithmic process used to derive Level 1 data from Level 0 data for soil heat flux is described in this document. This document does not provide computational implementation details, except for cases where these stem directly from algorithmic choices explained here.



Title: NEON Algorithm Theoretical Basis Document (ATBD): TIS Soil Heat Flux		Date: 02/05/2020
NEON Doc. #: NEON.DOC.000814	Author: N. Pingintha-Durden	Revision: B

## 2 RELATED DOCUMENTS, ACRONYMS AND VARIABLE NOMENCLATURE

### 2.1 Applicable Documents

AD[01]	NEON.DOC.000001	NEON OBSERVATORY DESIGN
AD[02]	NEON.DOC.005003	NEON Scientific Data Products Catalog
AD[03]	NEON.DOC.002652	NEON Level 1, Level 2 and Level 3 Data Products Catalog
AD[04]	NEON.DOC.005005	NEON Level 0 Data Products Catalog
AD[05]	NEON.DOC.000782	ATBD QA/QC Data Consistency
AD[06]	NEON.DOC.011081	ATBD QA/QC Plausibility Tests
AD[07]	NEON.DOC.000783	ATBD De-spiking and Time Series Analyses
AD[08]	NEON.DOC.000746	Calibration Fixture and Sensor Uncertainty Analysis (CVAL)
AD[09]	NEON.DOC.000785	TIS Level 1 Data Products Uncertainty Budget Estimation Plan
AD[10]	NEON.DOC.000751	CVAL Transfer of standard procedure
AD[11]	NEON.DOC.000927	NEON Calibration and Sensor Uncertainty Values <sup>1</sup>
AD[12]	NEON.FIU.011071	FIU Site Specific Sensor Location Matrix
AD[13]	NEON.DOC.001113	Quality Flags and Quality Metrics for TIS Data Products
AD[14]	NEON.DOC.002651	NEON Data Product Numbering Convention

<sup>1</sup> Note that CI obtains calibration and sensor values directly from an XML file maintained and updated by CVAL in real time. This report is updated approximately quarterly such that there may be a lag time between the XML and report updates.

### 2.2 Reference Documents

RD[01]	NEON.DOC.000008	NEON Acronym List
RD[02]	NEON.DOC.000243	NEON Glossary of Terms
RD[03]	HFP01SC Self Calibrating Heat Flux Sensor™ USER MANUAL HFP01SC Manual v0710	
RD[04]	Application and Specification of Heat Flux Sensors Version 9904	
RD[05]	Email correspondence with Jörgen Konings of Hukseflux (5 March 2014). K:\TIS Assemblies\22. Soil Heat Flux\Other Design Docs_Notes\Email correspondence with Jorgen.pdf	

### 2.3 Acronyms

Acronym	Explanation
---------	-------------

<sup>1</sup> Note that CI obtains calibration and sensor values directly from an XML file maintained and updated by CVAL in real time. This report is updated approximately quarterly such that there may be a lag time between the XML and report updates.

AIS	Aquatic Instrument System
ATBD	Algorithm Theoretical Basis Document
CI	NEON Cyberinfrastructure
CVAL	NEON Calibration, Validation, and Audit Laboratory
DAS	Data Acquisition System
DP	Data Product
FDAS	Field Data Acquisition System
FIU	Fundamental Instrument Unit
GRAPE	Grouped Remote Analog Peripheral Equipment
Hz	Hertz
L0	Level 0
L1	Level 1
QA/QC	Quality assurance and quality control
TIS	Terrestrial Instrument System

## 2.4 Variable Nomenclature

The symbols used to display the various inputs in the ATBD, e.g., calibration coefficients and uncertainty estimates, were chosen so that the equations can be easily interpreted by the reader. However, the symbols provided will not always reflect NEON’s internal notation, which is relevant for CI’s use, and or the notation that is used to present variables on NEON’s data portal. Therefore a lookup table is provided in order to distinguish what symbols specific variables can be tied to in the following document.

Symbol	Internal Notation	Description
$E_C$	CVALA0	Original correction factor ( $V/Wm^{-2}$ )
$R_s$	CVALA1	Resistance of a current-sensing resistor in series with the film resistor ( $\Omega$ )
$u_{A1}$	U_CVALA1	Combined, relative, calibration uncertainty provided in AD[11] (%)
$u_{A3}$	U_CVALA3	Combined, relative, calibration uncertainty (truth and trueness only); AD[11] (%)
$u_{V1}$	U_CVALV1	Combined, relative Field DAS uncertainty for voltage measurements; AD[11] (%)
$u_{V3}$	U_CVALV3	Combined, relative Field DAS uncertainty (truth and trueness only) for voltage measurements; AD[11] (%)
$O_V$	U_CVALV4	Offset imposed by the FDAS for voltage readings provided in AD[11] (V)



Title: NEON Algorithm Theoretical Basis Document (ATBD): TIS Soil Heat Flux		Date: 02/05/2020
NEON Doc. #: NEON.DOC.000814	Author: N. Pingintha-Durden	Revision: B

### 3 DATA PRODUCT DESCRIPTION

#### 3.1 Variables Reported

The soil heat flux related L1 DPs provided by the algorithms documented in this ATBD are displayed in the accompanying shf\_datapub\_NEONDOC003223.txt file.

#### 3.2 Input Dependencies

Table 3-1 details the soil heat flux related L0 DPs used to produce L1 DPs in this ATBD.

**Table 3-1: List of soil heat flux related L0 DPs that are transformed into L1 DPs in this ATBD.**

Description	Sample Frequency	Units	Data Product Number
Soil heat flux sensor voltage ( $V_s$ )	0.1 Hz	V	NEON.DOM.SITE.DP0.00040.001.01798.HOR.VER.000
Calibration Heater flags ( $F_H$ )	0.2 Hz	Binary (0/1)	NEON.DOM.SITE.DP0.00040.001.01799.HOR.VER.000
Voltage across the current sensing resistor ( $V_{cur}$ )	0.1 Hz	V	NEON.DOM.SITE.DP0.00040.001.01800.HOR.VER.000

#### 3.3 Product Instances

The soil heat flux data product will be available at NEON core and relocatable sites. At each core and relocatable site, soil heat flux sensors will be distributed within three of the five soil plots within the TIS soil array. The HFP01SC sensor will be installed below the soil surface at a depth specified in the geolocation data. A description of how the sensors are located within the plots is described in AD[12]. Individual instance of all HFP01SC-related L1 data products are in the accompanying shf\_datapub\_NEONDOC003223.txt file.

#### 3.4 Temporal Resolution and Extent

One- and thirty-minute averages of soil heat flux will be calculated to form L1 DPs.



Title: NEON Algorithm Theoretical Basis Document (ATBD): TIS Soil Heat Flux		Date: 02/05/2020
NEON Doc. #: NEON.DOC.000814	Author: N. Pingintha-Durden	Revision: B

### 3.5 Spatial Resolution and Extent

The soil heat flux measurement is spatially variable due to the small size of heat flux sensors relative to the scale of heterogeneity in surface conditions. A single measurement of soil heat flux is representative of the area of the sensor plate (Sauer and Horton, 2005). Therefore, replicate measurements are designed to be made across NEON’s soil array. To maximize spatial coverage, soil heat flux sensors will be deployed in three out of five soil plots that comprise the soil array at each core and relocatable site. Their measurements will be representative of the soil at the point that the HFP01SC sensors are deployed.

## 4 SCIENTIFIC CONTEXT

Soil heat flux, typically accessed in the vertical direction, is the amount of thermal energy that moves by conduction across an area of soil in a unit of time and usually expressed in Watts per square meter (Sauer and Horton, 2005). Soil heat flux is a key parameter in surface energy balance studies. Typically, soil heat flux is measured a few centimeters below the soil surface rather than directly at the surface (Ochsner et al., 2007). Heat flux at the surface is obtained by summing the flux at the measurement depth and the change in heat storage in the soil layer above the measurement depth.

### 4.1 Theory of Measurement

A heat flux plate is the most common sensor to measure soil heat flux. Heat flux sensors are typically small, rigid, disc-shape sensors that are inserted horizontally into the soil at the reference depth (Ochsner et al., 2006). An encapsulated thermopile in the sensor produces a voltage proportional to the temperature gradient perpendicular (e.g., vertical) across the sensor body (Ochsner et al., 2006). The material of the heat flux sensor mimics the bulk density and thermal heat diffusivities of a common loam soil. Assuming that the actual soil heat flux is at steady state, i.e., the thermal conductivity of the body is constant and that the sensor has negligible influence on the thermal flow pattern, the output voltage is directly proportional to the local/measured heat flux, see Figure 1.

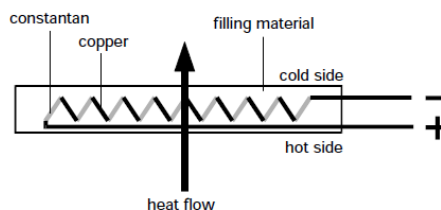


Figure 1. Conceptual schematic of a heat flux sensor (source: RD [04]).



Biases when using heat flux plates to measure soil heat flux can arise from both temperature differences and thermal conductivity differences between the sensor and soil. Typical heat flux sensors do not correct for this bias, as a result soil heat flux estimates are often under/overestimated (See Sections 6.1.1 through 6.1.3). The HFP01SC sensor self-calibrates using the Van den Bos-Hoeksema method to account, under empirical conditions, for these errors (RD[03]).

The HFP01SC sensor self-calibrates using the Van den Bos-Hoeksema method via a film heater mounted on top of the heat flux sensor. When the heater is activated, half of the heat flux would pass upward into the surrounding medium and half would pass downward through the plate. In an ideal case, the heat flux through the plate would be one half of the heating power. In reality, for a self-calibrating plate installed in soil, the actual flux through the plate caused by heating will generally not be equal to half of the heating power. The ratio of the ideal to actual flux is a measure of heat flow distortion during heating (Ochsner et al, 2006; RD[03]). The heat flow distortion during heating is then compared to the heat flow distortion under ambient conditions (measured when the heater is off) and is used to correct for the deflection error (Ochsner et al, 2006; RD[03]).

## 4.2 Theory of Algorithm

Given the caveats mentioned above, if the heat flux is assumed to be in a steady state, the signal of HFP01SC (in volt) is proportional to the local heat flux in  $W\ m^{-2}$  (RD [03]). To perform a self-calibration and estimate the *in-situ* correction factor, the sensor will self-calibrate at regular intervals as defined in AD[09]. Self-calibration consists of applying 12 V to the film heater for 180 s to generate a heat pulse (Figure 2). The plate's response to the self-heating ( $V_a$ ) is quantified by:

$$V_a = V_s(t_{180}) - \left( \left( \left( \frac{V_s(t_c) - V_s(t_0)}{t_c - t_0} \right) \cdot (t_{180} - t_0) \right) + V_s(t_0) \right) \quad (1)$$

where:

$V_a$  = Sensor's response to self-heating (V)

$V_s(t_0)$  = Output from the sensor at start time of calibration period (V)

$V_s(t_{180})$  = Output from the sensor at 180 s after the initiation of heat pulse (V)

$V_s(t_c)$  = Output from the sensor at time  $c$  after the initiation of the heat pulse (signaling the end of a calibration period; V)



Note that the calibration interval was initially set to 3.25 h and subsequently changed to 13 h in 2020; however, this values is subject to further change. In addition, the duration of the entire calibration period ( $t_c$ ) may be changed depending on soil type.

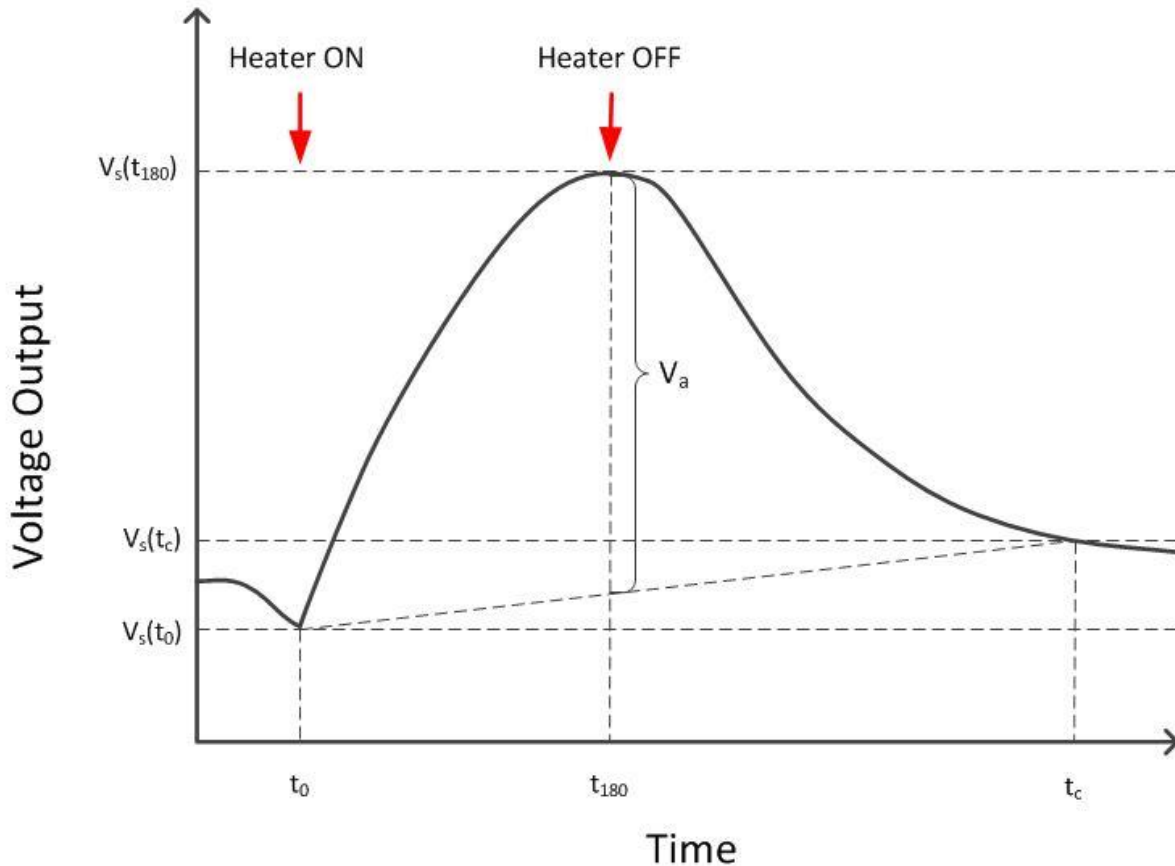


**Figure 2.** A conceptual plot of the voltage output ( $V_s$ ) from the sensor when performing a self-calibration.

After the sensor response to self-heating ( $V_a$ ) is obtained, the *in-situ* correction factor ( $E_f$ ;  $V/Wm^{-2}$ ) for the plate is then estimated as:

$$E_f = 2V_a \left[ \frac{R_r^2 A_s}{V_{cur}^2 R_s} \right] \quad (2)$$

where:  $R_r$  = Resistance of a current-sensing resistor in series with the film resistor ( $\Omega$ ; constant at 5  $\Omega$ )



$V_{cur}$  = Voltage across the current sensing resistor (V; output at 180 s after the initiation of heat pulse)

$A_s$  = Surface area of the plate (m<sup>2</sup>; constant at 0.003885 m<sup>2</sup>)

$R_s$  = Resistance of the film resistor ( $\Omega$ )

The constant value of  $R_r$  will be provided by ENG, while  $A_s$  and  $R_s$  is given by the manufacturer. These constant values will be provided by FIU and maintained in the CI data store. The *in-situ* correction factor is updated after every *in-situ* calibration.

Once the *in-situ* correction factor is resolved, soil heat flux can be determined by

$$\varphi = \frac{V_s}{E_f} \quad (3)$$

where:

$\varphi$  = soil heat flux (W m<sup>-2</sup>)

$V_s$  = Output signal from the plate during measurement period (V)

$E_f$  = *In-situ* correction factor (V/Wm<sup>-2</sup>)

After soil heat flux ( $\varphi$ ) is determined, one-minute ( $\varphi_{1min}$ ) and thirty-minute ( $\varphi_{30min}$ ) averages will be determined accordingly to create L1 data products:

$$\varphi_{1min} = \frac{1}{n} \sum_{i=1}^n \varphi_i \quad (4)$$

where, for each minute average,  $n$  is the number of measurements during the averaging period and  $\varphi_i$  is 0.1 Hz soil heat flux measurement taken during the 60-second averaging period [0, 60). For a 1-minute average,  $n = 6$  if all data points are included, and

$$\varphi_{30min} = \frac{1}{n} \sum_{i=1}^n \varphi_i \quad (5)$$

where, for each thirty-minute average,  $n$  is the number of measurements during the averaging period - and  $\varphi_i$  is 0.1 Hz soil heat flux measurement taken during the 1800-second averaging period [0, 1800).

Note: The beginning of the first averaging period in a series shall be the nearest whole minute less than or equal to the first timestamp in the series.



Title: NEON Algorithm Theoretical Basis Document (ATBD): TIS Soil Heat Flux		Date: 02/05/2020
NEON Doc. #: NEON.DOC.000814	Author: N. Pingintha-Durden	Revision: B

#### 4.2.1 Time regularization

The measurement frequency of soil heat flux sensor voltage ( $V_s$ ), voltage across the current sensing resistor ( $V_{cur}$ ), and calibration heater flags ( $F_H$ ) are different (see details in Table 3-1). To be able to align all measurements in Table 3-1, each associated time stamp shall always be rounded to the full second with 10 s increment as:

$$ss = \begin{cases} x \text{ if } x - 5 \leq ss < x + 5 \text{ where } x = 10, 20, 30, 40, \text{ and } 50 \\ 00, \text{ otherwise} \end{cases} \quad (6)$$

where,  $ss$  is second in timestamp.

Note that the latest data will be selected if there are more than one data found in 10 s window.

## 5 ALGORITHM IMPLEMENTATION

Data flow for signal processing of L1 data products will be treated in the following order.

1. Regularize timestamp as described in section 4.2.1.
2. Initially, soil heat flux ( $W\ m^{-2}$ ) will be determined according to Eq. (3) as described in section 4.2. using the original correction factor ( $E_C$ ) given by the manufacturer. If the calibration heater flag LO data streams are missing, soil heat flux will be calculated using  $E_C$ .
3. Assign the calibration heater flag ( $F_H$ ) = '1' to 0.1 Hz data if the heater for *in-situ* self-calibration is turned on, otherwise  $F_H$  = '0'. The details are provided below.
4. Assign the calibration period flag ( $F_{Cal}$ ) = '1' to 0.1 Hz data collected during the calibration period, otherwise  $F_{Cal}$  = '0'. The details are provided below.
5. During the calibration period, once the calibration heater is turned off, determine and assign the calibration heater quality flag ( $QF_H$ , i.e. '0' if the calibration heater is turned on correctly and '1' if the calibration heater is failed to turn on) to 0.1 Hz data collected thereafter until the next *in-situ* self-calibration is performed. The  $QF_H$  will be determined using Eq. (7).
6. After every *in-situ* self-calibration processes are done, the *in-situ* correction factor will be determined according to Eq. (1) and (2).
7. Determine and assign the *in-situ* correction quality flag ( $QF_{EF}$ , i.e. '0' if there is no error and '1' if error is detected during the calibration) to 0.1 Hz data collected thereafter until the next *in-situ* self-calibration is performed. The  $QF_{EF}$  will be determined using Eq. (8).



8. Soil heat flux ( $W\ m^{-2}$ ) will be determined using Eq. (3). The updated *in-situ* correction factor will be applied to the 0.1 Hz data collected thereafter until the next *in-situ* self-calibration is performed.
9. For the 0.1 Hz data that have  $QF_{EF} = '1'$  associated with its timestamp, soil heat flux will be calculated using the original correction factor ( $E_C$ ) given by the manufacturer.
10. QA/QC Plausibility tests will be applied to the data stream in accordance with AD[06]. The details are provided below.
11. Signal de-spiking and time series analysis will be applied to the data stream in accordance with AD[07].
12. One- and thirty-minute soil heat flux averages will be calculated using Eq. (4) and (5) and descriptive statistics (i.e. minimum, maximum, and variance) will be determined for both averaging periods.
13. Quality metrics, quality flags, and the final quality flag will be produced for one-, and thirty-minute averages according to AD[13]. However, for the following flags,  $F_H$ ,  $F_{Cal}$ ,  $QF_H$ , and  $QF_{EF}$ , if one or more of high flags ('1') are detected over the averaging period, set that flag to '1' for the whole averaging period.

#### QA/QC Procedure:

1. **Plausibility Tests** AD[06] – All plausibility tests will be determined for soil heat flux. Test parameters will be provided by FIU and maintained in the CI data store. All plausibility tests will be applied to the sensor's converted LO DP and an associated pass/fail flag will be generated for each test. Note that the step test will not be run when the calibration period flag ( $F_{Cal}$ ) is set high.
2. **Sensor test** – Flags will be generated for the sensor tests which include, the calibration heater flag ( $F_H$ ), the calibration heater quality flag ( $QF_H$ ), the calibration period flag ( $F_{Cal}$ ), and the in-situ correction quality flag ( $QF_{EF}$ ), which are defined below. These flags will be generated as part of the L1 data products and maintained in the CI data store. One- and thirty-minute averages of quality metrics of the these flags will be produced according to AD[13].
  - a. Calibration heater flag ( $F_H$ ) is derived from the LO data products and is identified in the C<sup>3</sup> document (AD[09]). The calibration heater flag indicates the sensor is turned on to perform a self-calibration. The calibration heater flag shall read '0' under normal operating conditions and '1' when the sensor is self-calibrating. Any LO DP (i.e., 0.1 Hz data) that has a calibration heater flag associated with its timestamp will not be used to compute soil heat flux (sensor's converted LO DP).
  - b. Calibration heater quality flag ( $QF_H$ ) will be generated as part of the L1 data product to determine that the calibration heater is turned on correctly,  $QF_H = '0'$ , and  $QF_H = '1'$  when the calibration heater is failed to turn on. The calibration heater quality flag will be determined as follows:



Title: NEON Algorithm Theoretical Basis Document (ATBD): TIS Soil Heat Flux		Date: 02/05/2020
NEON Doc. #: NEON.DOC.000814	Author: N. Pingintha-Durden	Revision: B

$$QF_H = \begin{cases} 1 & \text{if } F_H = 1 \text{ and } [V_s(t_{180}) - V_s(t_0)] < d \cdot |V_s(t_c) - V_s(t_0)| \\ 0 & \text{otherwise.} \end{cases} \quad (7)$$

where,  $d$  is the calibration heater quality flag threshold and set as default at 5.

Since the calibration heater quality flags are generated after the calibration heater is turned off, a specific calibration heater quality flag will be associated with the 0.1 Hz data collected after the preceding calibration heater quality flag.

- c. Calibration period flag ( $F_{Cal}$ ) will be generated as part of the L1 data product to indicate the calibration period for the sensor. The calibration period flag shall read '0' under normal operating conditions and '1' under calibration period. This period starts at the time the heater is turned on at  $t_0$  and ends at  $t_c$ . Any L0 DP (i.e., 0.1 Hz data) that has a calibration heater flag associated with its timestamp will not be used to compute soil heat flux (sensor's converted L0 DP).
- d. In-situ correction flag ( $QF_{EF}$ ) will be generated as part of the L1 data product to indicate that an error occur during the calibration process (i.e. '0' if there is no error and '1' if error is detected). Errors can arise in the *in-situ* calibration process if there is too much fluctuation between the heat flux in the soil during the calibration process (RD [03]). Since the *in-situ* correction quality flags are generated after *in-situ* self-calibration processes are done, a specific *in-situ* correction quality flag will be associated with the 0.1 Hz converted L0 DPs collected after the preceding *in-situ* correction quality flag. The *in-situ* correction quality flag will be determined as follows:

$$QF_{EF} = \begin{cases} 1 & \text{if } E_f > (a * E_C) \text{ Or } E_f < (b * E_C) \text{ Or } |V_s(t_0) - V_s(t_c)| > cV_a \text{ Or } QF_H = 1 \\ 0 & \text{otherwise} \end{cases} \quad (8)$$

where:  $E_C$  = Original correction factor given by the manufacturer (provided by FIU and maintained in the CI data store;  $V/Wm^{-2}$ )

$a$ ,  $b$ , and  $c$  = *In-situ* correction quality flag thresholds; default value of  $a = 1.20$ ,  $b = 0.5$ , and  $c = 0.1$ .



Title: NEON Algorithm Theoretical Basis Document (ATBD): TIS Soil Heat Flux		Date: 02/05/2020
NEON Doc. #: NEON.DOC.000814	Author: N. Pingintha-Durden	Revision: B

3. **Signal Despiking** – The time series despiking routine will be run according to AD[07]. Test parameters will be specified by FIU and maintained in the CI data store. Quality flags resulting from the despiking analysis will be applied according to AD[07]. Note that this test will not be run when the calibration period flag ( $F\_Cal$ ) is set high.
4. **Quality Flags (QFs) and Quality Metrics (QMs)** – If a datum has failed one of the following test it will not be used to create a L1 DP, range, persistence, step,  $F\_H$ , and  $F\_Cal$ .  $\alpha$  and  $\beta$  QFs and QMs will be determined using the flags listed in Table 5-1. In addition, L1 DPs will have a QA/QC report and quality metrics associated with each flag listed in Table 5-1 as well as a final quality flag ( $finalQF$ ), as detailed in AD[13]. Ancillary information needed for the algorithm and other information maintained in the CI data store is shown in Table 5-2.

**Table 5-1: Flags associated with soil heat flux measurements.**

<b>Tests</b>
Range
Persistence
Step
Null
Gap
Signal De-spiking
Calibration period flag
<i>In-situ</i> correction flag
Alpha
Beta
Final Quality Flag

**Table 5-2: Information maintained in the CI data store for with soil heat flux measurements.**

Tests/Values	CI Data Store Contents
Range	Minimum and maximum values



Title: NEON Algorithm Theoretical Basis Document (ATBD): TIS Soil Heat Flux		Date: 02/05/2020
NEON Doc. #: NEON.DOC.000814	Author: N. Pingintha-Durden	Revision: B

Tests/Values	CI Data Store Contents
Persistence	Window size, threshold values and maximum time length
Step	Threshold values
Null	Test limit
Gap	Test limit
Signal Despiking	Time segments and threshold values
Uncertainty	AD[08]
Sensor Specifications	$R_r$ provided by ENG and $A_s$ , $R_s$ , and $E_c$ provided by the manufacture
Final Quality Flag	AD[13]

## 6 UNCERTAINTY

Uncertainty of measurement is inevitable (ISO 1995; Taylor 1997). It is imperative that uncertainties are identified and quantified to determine statistical interpretations about mean quantity and variance structure; both are needed to construct higher level data products (i.e., L1 DP, etc.) and modeled processes. This portion of the document serves to identify, evaluate, and quantify sources of uncertainty relating to L1 soil heat flux DPs. It is a reflection of the information described in AD[10], and is explicitly described for the Soil Heat Flux assembly in the following sections.

### 6.1 Uncertainty of Soil Heat Flux Measurements

Uncertainty of the soil heat flux assembly is discussed in this section. Sources of uncertainties include those arising from thermal conductivity (i.e., soil moisture) differences, temperature dependence, the sensor’s self-calibration procedure, and measurement noise introduced by the data acquisition system. It should be noted that CVAL will not calibrate the soil heat flux sensors, as the sensors are programmed to conduct regularly scheduled self-calibrations (refer to Section 4.2).



### 6.1.1 Measurement Uncertainty

The following subsections present the uncertainties associated with *individual observations*. It is important to note that the uncertainties presented in the following subsections are *measurement uncertainties*, that is, they reflect the uncertainty of an *individual* measurement. These uncertainties should not be confused with those presented in Section 6.1.2. We urge the reader to refer to AD[10] for further details concerning the discrepancies between quantification of measurement uncertainties and temporally averaged data product uncertainties.

NEON calculates measurement uncertainties according to recommendations of the Joint Committee for Guides in Metrology (JCGM) 2008. In essence, if a measurand  $y$  is a function of  $n$  input quantities

$x_i$  ( $i = 1, \dots, n$ ), *i.e.*,  $y = f(x_1, x_2, \dots, x_n)$ , the combined measurement uncertainty of  $y$ , assuming the inputs are independent, can be calculated as follows:

$$u_c(y) = \left( \sum_{i=1}^N \left( \frac{\partial f}{\partial x_i} \right)^2 u^2(x_i) \right)^{\frac{1}{2}} \quad (9)$$

where

$\frac{\partial f}{\partial x_i}$  = partial derivative of  $y$  with respect to  $x_i$

$u(x_i)$  = combined standard uncertainty of  $x_i$ .

Thus, the uncertainty of the measurand can be found by summing the input uncertainties in quadrature.

#### 6.1.1.1 Thermal conductivity and temperature dependence

The thermal conductivity of the HFP01SC is  $0.8 \text{ W m}^{-1} \text{ K}^{-1}$  (RD[03]), while that of soil can vary from  $0.2$  (dry) to  $4.0 \text{ W m}^{-1} \text{ K}^{-1}$  (saturated). The discrepancy between the thermal conductivity of the soil heat flux sensor and that of the surrounding soil causes a thermal conductivity (or deflection) error. It is shown that this discrepancy can cause soil heat flux underestimates up to  $-16\%$  of the expected measurement reading (RD[03]).

The HFP01SC is also prone to errors arising from temperature differences between the soil and the heat flux plate. These can be as large as  $\pm 5\%$  of the measurand if the sensor is left uncalibrated (RD[03]).



Title: NEON Algorithm Theoretical Basis Document (ATBD): TIS Soil Heat Flux		Date: 02/05/2020
NEON Doc. #: NEON.DOC.000814	Author: N. Pingintha-Durden	Revision: B

### 6.1.1.2 In-situ self-calibration

Before a HFP01SC is shipped from Hukseflux to a customer, the sensor is calibrated to an ISO traceable “guarded hot plate.” Once deployed in the field, the sensor is programmed to undergo self-calibrations at user-defined time intervals (See Section 4). If the sensor is successfully self-calibrated in the field, the thermal conductivity and temperature errors are corrected to *within ± 3% accuracy relative to the ISO traceable “guarded hot plate”* (RD[03]). This situation illustrates a pitfall, in that, the accuracy of soil heat flux measurements is quantified relative to a material that is not representative of soils. Because of this, the end-user should be cognizant that even in the event that the HFP01SC completes a successful in-situ self-calibration in the field, the resulting measurement uncertainty with respect to calibration is at minimum *± 3% accuracy relative to the ISO traceable “guarded hot plate.”* This estimate is crude at best and is possibly underestimated relative to field conditions.

**Note:** Hukseflux uses the term *accuracy* to represent measurement *uncertainty*, and such values are given at 95% confidence throughout the manual (RD[05]).

To convert this expanded, relative uncertainty to an unexpanded, standard uncertainty, i.e., one that is given at a single confidence interval and is in units of measurement, Eq. (10) is used.

$$u_{CAL}(\varphi_i) = u_{A1} * \varphi_i \quad (10)$$

Where,

- $u_{CAL}(\varphi_i)$  = standard calibration uncertainty of an individual measurement (W m<sup>2</sup>)
- $u_{A1}$  = relative, calibration uncertainty provided in AD[11] (%)
- $\varphi_i$  = individual, soil heat flux measurement (W m<sup>2</sup>)

### 6.1.1.3 Field DAS

The Field DAS (FDAS) introduces noise to the analog signals  $V_s$  and  $V_{cur}$ . This uncertainty is quantified via:

$$u_{FDAS}(X_i) = (u_{V1} * X_i) + O_V \quad (11)$$

Where:

- $u_{FDAS}(X)$  = standard uncertainty of the voltage measurement introduced by the Field DAS (V)
- $X_i$  = voltage measurement, either  $V_s$ , or  $V_{cur}$  (V)



- $u_{V1}$  = combined, relative Field DAS uncertainty for voltage measurements provided by CVAL in AD[11] (unitless)
- $O_V$  = offset imposed by the FDAS for voltage readings, provided by CVAL (V)

The uncertainty introduced by the FDAS ultimately propagates to the soil heat flux measurement  $\phi$ . Here, we detail this process in a few steps. First, we derive a combined uncertainty for  $V_a$ , which equals  $f(V_s(t_0), V_s(t_{180}), V_s(t_c))$ .

The partial derivatives of the sensor's response to self-heating  $V_a$ , with respect to the appropriate voltage reading are:

$$\frac{\partial V_a}{\partial V_{s(t_c)}} = \frac{t_{180} - t_0}{t_0 - t_c} \quad (12)$$

$$\frac{\partial V_a}{\partial V_{s(t_0)}} = \frac{t_c - t_{180}}{t_0 - t_c} \quad (13)$$

$$\frac{\partial V_a}{\partial V_{s(t_{180})}} = 1 \quad (14)$$

The uncertainty of a voltage measurement  $V_{s(t)}$ , due to the FDAS is:

$$u_{FDAS V_{s(t)}}(V_a) = \left| \frac{\partial V_a}{\partial V_{s(t)}} \right| u_{FDAS}(V_{s(t)}) \quad (15)$$

where:

$$\frac{\partial V_{a_i}}{\partial V_{s(t)}} = \text{partial derivative of Eq. (1) with respect to } V_{s(t)} \text{ (V)}$$

$$u_{FDAS V_{s(t)}}(V_a) = \text{standard uncertainty of measurement introduced by the Field DAS (V)}$$



The combined uncertainty of  $V_a$  is then:

$$u_c(V_a) = \left( u_{FDASV_s(t_0)}^2(V_a) + u_{FDASV_s(t_{180})}^2(V_a) + u_{FDASV_s(t_c)}^2(V_a) \right)^{\frac{1}{2}} \quad (16)$$

Next, the partial derivatives of the soil heat flux measurement  $\varphi$ , with respect to  $V_s$ ,  $V_{cur}$ , and  $V_a$  are derived. It should be noted that  $V_s$  (Eq. (3)) and all  $V_s(t)$  (Eq. (1)) are independent, as all  $V_s(t)$  (Eq. (1)) are only valid during the calibration period, while measurements of  $V_s$  (Eq. (3)) are only valid outside of the calibration period.

Substituting Eq. (2) into Eq. (3) and rearranging the terms we get:

$$\varphi = \frac{V_s}{E_f} = \frac{R_s V_{cur}^2 V_s}{2A_s R_r^2 V_a} \quad (17)$$

The partial derivatives of Eq. (17) with respect to  $V_{cur}$ ,  $V_a$ , and  $V_s$  are shown below.

$$\frac{\partial \varphi}{\partial V_{cur}} = \frac{R_s V_{cur} V_s}{A_s R_r^2 V_a} \quad (18)$$

$$\frac{\partial \varphi}{\partial V_s} = \frac{R_s V_{cur}^2}{2A_s R_r^2 V_a} \quad (19)$$

$$\frac{\partial \varphi}{\partial V_a} = -\frac{R_s V_{cur}^2 V_s}{2A_s R_r^2 V_a^2} \quad (20)$$

The partial uncertainties are thus:

$$u_{FDASV_{cur}}(\varphi_i) = \left| \frac{\partial \varphi}{\partial V_{cur}} \right| u_{FDAS}(V_{cur}) \quad (21)$$



$$u_{FDASV_s}(\varphi_i) = \left| \frac{\partial \varphi}{\partial V_s} \right| u_{FDAS}(V_{s_i}) \quad (22)$$

$$u_{FDASV_a}(\varphi_i) = \left| \frac{\partial \varphi}{\partial V_a} \right| u_c(V_a) \quad (23)$$

#### 6.1.1.4 Combined Measurement Uncertainty

The combined, standard, measurement uncertainty of an individual soil heat flux measurement  $u_c(\varphi_i)$ , given in units of  $W m^{-2}$ , is computed by summing the individual uncertainties in quadrature:

$$u_c(\varphi_i) = \left( u_{CAL}^2(\varphi_i) + u_{FDASV_{cur}}^2(\varphi_i) + u_{FDASV_s}^2(\varphi_i) + u_{FDASV_a}^2(\varphi_i) \right)^{\frac{1}{2}} \quad (24)$$

If the self-calibration process is unsuccessful (refer to Section 4.2), the errors mentioned in Section 6.1.1 can collectively over- or under-estimate measurements. In the event of an unsuccessful calibration, data will be flagged ( $QF\_EF$ ), and soil heat flux will be calculated using the original correction factor ( $E_C$ ) given by the manufacturer. Uncertainty estimates will only comprise the manufacturer default uncertainty,  $u_{CAL}(\varphi_i)$ . The user should exercise caution when using any data where the manufacturer calibration coefficients are applied.

Given that the NEON Observatory will be monitoring both soil temperature and soil water content, it is theoretically possible to derive the thermal conductivity and temperature of the soil surrounding the heat flux sensor. Thus, if the self-calibration is unsuccessful, it may be possible to correct for the unavoidable errors caused by temperature and thermal conductivity discrepancies. This subject will need to be investigated in the future as NEON data are collected and analyzed.

#### 6.1.1.5 Expanded Measurement Uncertainty

The expanded measurement uncertainty is calculated as:

$$U_{95}(\varphi_i) = k_{95} * u_c(\varphi_i) \quad (25)$$

Where:

$$U_{95}(\varphi_i) = \text{expanded measurement uncertainty at 95\% confidence (} W m^{-2} \text{)}$$



Title: NEON Algorithm Theoretical Basis Document (ATBD): TIS Soil Heat Flux		Date: 02/05/2020
NEON Doc. #: NEON.DOC.000814	Author: N. Pingintha-Durden	Revision: B

$k_{95}$  = 2; coverage factor for 95% confidence (unitless)

## 6.1.2 Uncertainty of L1 Mean Data Product

The following subsections discuss uncertainties associated with temporally averaged, i.e., L1 mean, data products. As stated previously, it is important to note the differences between the *measurement uncertainties* presented in Section 6.1.1 and the uncertainties presented in the following subsections. The uncertainties presented in the following subsections reflect the uncertainty of a time-averaged mean value, that is, they reflect the uncertainty of a distribution of measurements collected under non-controlled conditions (i.e., those found in the field), as well as any uncertainties, in the form of *Truth* and *Trueness*, related to the accuracy of the field assembly.

### 6.1.2.1 Repeatability (natural variation)

To quantify the uncertainty attributable to random effects, the distribution of the individual measurements is used. Specifically, the *estimated standard error of the mean (natural variation)* is computed. This value reflects the repeatability of insolation measurements for a specified time period:

$$u_{NAT}(\bar{\varphi}) = \frac{s(\varphi)}{\sqrt{n}} \quad (26)$$

Where,

$u_{NAT}(\bar{\varphi})$  = standard error of the mean (natural variation) (W m<sup>-2</sup>)

$s(\varphi)$  = experimental standard deviation of individual observations for the defined time period (W m<sup>-2</sup>)

$n$  = number of observations made during the defined time period. (unitless)

### 6.1.2.2 Calibration

At NEON's CVAL, uncertainty budgets are partitioned by components of uncertainty, e.g., repeatability, reproducibility, and trueness. For many of NEON's L1 DP, the uncertainty resulting from sensor calibration that propagates to the L1 mean, DP is representative of measurement trueness and omits the repeatability and reproducibility. Repeatability and reproducibility of the L1 mean values are then



Title: NEON Algorithm Theoretical Basis Document (ATBD): TIS Soil Heat Flux		Date: 02/05/2020
NEON Doc. #: NEON.DOC.000814	Author: N. Pingintha-Durden	Revision: B

quantified via the standard deviation of the mean (see Section 6.1.2.1). Unlike many of the sensors deployed throughout the NEON observatory, the soil heat flux sensors are not calibrated at NEON’s CVAL before field deployment. The sensors are calibrated by Hukseflux and undergo self-calibrations once deployed in the field. Hukseflux does not provide individual estimates of trueness, repeatability, or reproducibility, rather, the vendor assigns an expanded uncertainty of  $\pm 3\%$  to calibrated soil heat flux measurements (RD[03]). The *unexpanded* uncertainty provided by Hukseflux propagates to the combined uncertainty of the L1, mean DP.

$$u_{CAL}(\bar{\varphi}) = u_{A3} * \bar{\varphi} \tag{27}$$

Where,

- $u_{CAL}(\bar{\varphi})$  = standard calibration uncertainty of a L1, mean, soil heat flux DP (W m<sup>2</sup>)
- $u_{A3}$  =  $u_{A1}$  (%)
- $\bar{\varphi}$  = L1, mean soil heat flux DP (W m<sup>2</sup>)

The decision to use the entire uncertainty estimate for the L1, mean data product can be philosophically debated. On one hand, it can be argued that this approach results in double-counting of repeatability and reproducibility. However, the magnitude of the natural variation of the L1, mean DP will most likely override the uncertainty estimate provided by Hukseflux. On the other hand, it can be argued that regardless of which term is propagated, i.e., measurement trueness only or the overall uncertainty, the uncertainty estimate provided by Hukseflux is most likely an underestimate of the uncertainty for the soil heat flux plate in soil (as opposed to the “guarded hot plate”).

### 6.1.2.3 Field DAS

Since the L1 mean soil heat flux DP is a function of the individual soil heat flux measurements, any measurement *bias* introduced by the Field DAS will be reflected in the L1 mean data product. Here, the raw measurements of  $V_{cur}$  and  $V_s$  that maximize the combined uncertainty of an individual measurement (Eq. (24)) are used in the calculation of the L1 mean DP uncertainty. Uncertainty components due to random effects, whether a function of the environment or the measurement assembly, are quantified via the natural variation of the mean (see Section 6.1.2.1). For more information regarding the justification of this approach, please see AD[10].

The accuracy of the Field DAS in the form of *Truth* and *Trueness* propagates through to the uncertainty of the mean DP similarly to how the Field DAS uncertainties associated with a raw resistance and a raw



voltage propagate through to the uncertainties of the measurement attributable to the Field DAS resistance and voltage readings.

$$u_{FDAS(TT)}(X_{MAX}) = (u_{V3} * X_{MAX}) + O_V \quad (28)$$

Where,

$u_{FDAS(TT)}(X_{MAX})$  = FDAS truth and trueness uncertainty of voltage measurement  $X$

$X_{MAX}$  = measurements corresponding to the MAX index (V)

$u_{V3}$  = relative, combined, Field DAS *Truth* and *Trueness* uncertainty for voltage measurements, provided by CVAL (unitless)

Where, the subscript “MAX” represents the index,  $i$ , where the *maximum*, combined, standard, measurement uncertainty of an individual soil heat flux measurement is observed over a set (averaging period) of observations. Mathematically, this can be defined as:

$$MAX = \{i: u_c(\varphi_i) = \max[u_c(\varphi_1), \dots, u_c(\varphi_n)]\}. \quad (29)$$

Thus, from Eq. (21) through (22):

$$u_{FDAS(TT)V_{cur}}(\bar{\varphi}) = \left| \frac{\partial \varphi}{\partial V_{cur}} \right| u_{FDAS(TT)}(V_{cur}) \quad (30)$$

**Note:**  $V_{cur}$  is observed at 180 seconds after the initiation of heat pulse (during calibration cycle). As such,  $V_{cur}$  from the most recent calibration cycle shall be used in Eq. (30)

$$u_{FDAS(TT)V_s}(\bar{\varphi}) = \left| \frac{\partial \varphi}{\partial V_s} \right|_{V_{sMAX}} u_{FDAS(TT)}(V_{sMAX}) \quad (31)$$

where



$$\left. \frac{\partial \varphi}{\partial V_{cur}} \right| = \text{partial derivative of } \varphi \text{ with respect to } V_{cur} \text{ (Eq. (18)); } \text{W m}^{-2} \text{V}^{-1}$$

$$\left. \frac{\partial \varphi}{\partial V_s} \right|_{V_{sMAX}} = \text{partial derivative of } \varphi \text{ with respect to } V_s \text{ (Eq. (19)) evaluated at } V_{sMAX} \text{ (W m}^{-2} \text{V}^{-1})$$

Because  $V_s(t_0)$ ,  $V_s(t_{180})$ , and  $V_s(t_c)$  are measurements pertaining only to self-calibration, the bias of these measurements that is introduced by the DAS will be quantified during the calibration period and not when the maximum combined uncertainty of an individual measurement  $\varphi_i$ , is observed. Thus, the following equations are used:

$$u_{FDAS(TT)}(V_{s(t)}) = (u_{V3} * V_{s(t)}) + O_V \quad (32)$$

$$u_{FDAS(TT)V_{s(t)}}(V_a) = \left| \frac{\partial V_a}{\partial V_{s(t)}} \right| u_{FDAS(TT)}(V_{s(t)}) \quad (33)$$

$$u_c(V_a) = \left( u_{FDAS(TT)V_{s(t_0)}}^2(V_a) + u_{FDAS(TT)V_{s(t_{180})}}^2(V_a) + u_{FDAS(TT)V_{s(t_c)}}^2(V_a) \right)^{\frac{1}{2}} \quad (34)$$

$$u_{FDAS(TT)V_a}(\bar{\varphi}) = \left| \frac{\partial \varphi}{\partial V_a} \right| u_c(V_a) \quad (35)$$

#### 6.1.2.4 Combined Uncertainty

The combined uncertainty for the L1, mean, soil heat flux data product,  $u_c(\bar{\varphi})$ , given in units of  $\text{W m}^{-2}$ , is computed by summing the uncertainties from Sections 6.1.2.1 through 6.1.2.3 in quadrature:



$$u_c(\bar{\varphi}) = \left( u_{CAL}^2(\bar{\varphi}) + u_{NAT}^2(\bar{\varphi}) + u_{FDAS(TT)_{V_{cur}}}^2(\bar{\varphi}) + u_{FDAS(TT)_{V_s}}^2(\bar{\varphi}) + u_{FDAS(TT)_{V_d}}^2(\bar{\varphi}) \right)^{\frac{1}{2}} \quad (36)$$

In the event of an unsuccessful calibration, data will be flagged (*QF\_EF*), and soil heat flux will be calculated using the original correction factor ( $E_C$ ) given by the manufacturer. Uncertainty estimates will only comprise the manufacturer default uncertainty,  $u_{CAL}(\varphi_i)$ . The user should exercise caution when using any data where the manufacturer calibration coefficients are applied.

Note that the combined uncertainty of soil heat flux which calculated using the original correction factor given by the manufacturer will be computed by accounting the uncertainties from  $u_{NAT}(\bar{\varphi})$  and  $u_{CAL}(\bar{\varphi})$ .

### 6.1.2.5 Expanded Uncertainty

The expanded uncertainty is calculated as:

$$U_{95}(\bar{\varphi}) = k_{95} * u_c(\bar{\varphi}) \quad (37)$$

Where:

$U_{95}(\bar{\varphi})$  = expanded L1 mean data product uncertainty at 95% confidence (W m<sup>-2</sup>)

$k_{95}$  = 2; coverage factor for 95% confidence (unitless)

## 6.2 Uncertainty Budget

The uncertainty budget is a visual aid detailing i) quantifiable sources of uncertainty, ii) means by which they are derived, and iii) the order of their propagation. Uncertainties denoted in this budget are either derived within this document or will be provided by other NEON teams (e.g., CVAL) and stored in the CI data store.

**Table 6-1: Uncertainty budget for individual soil heat flux measurements. Shaded rows denote the order of uncertainty propagation (from lightest to darkest).**



Source of measurement uncertainty	measurement uncertainty component $u(x_i)$	measurement uncertainty value [W m <sup>-2</sup> ]	$\frac{\partial f}{\partial x_i}$	$u_{x_i}(Y) \equiv \left  \frac{\partial f}{\partial x_i} \right  u(x_i)$ [W m <sup>-2</sup> ]
Soil heat flux	$u_c(\varphi_i)$	Eq. (24)	n/a	n/a
Traceable calibration	$u_{CAL}(\varphi_i)$	Eq. (10)	n/a	Eq. (10)
FDAS (signal)	$u_{FDAS}(V_{cur_i})$	Eq. (11) [V]	Eq. (18)	Eq. (21)
FDAS (signal)	$u_{FDAS}(V_{s_i})$	Eq. (11) [V]	Eq. (19)	Eq. (22)
In-situ cal. FDAS	$u_c(V_a)$	Eq. (16) [V]	Eq. (20)	Eq. (23)
FDAS (signal)	$u_{FDAS}(V_s(t_0))$	Eq. (11) [V]	Eq. (12)	Eq. (15)
FDAS (signal)	$u_{FDAS}(V_s(t_{180}))$	Eq. (11) [V]	Eq. (13)	Eq. (15)
FDAS (signal)	$u_{FDAS}(V_s(t_c))$	Eq. (11) [V]	Eq. (14)	Eq. (15)

**Table 6-2: Uncertainty budget for L1 mean soil heat flux DPs. Shaded rows denote the order of uncertainty propagation (from lightest to darkest).**

Source of uncertainty	uncertainty component $u(x_i)$	uncertainty value [W m <sup>-2</sup> ]	$\frac{\partial f}{\partial x_i}$	$u_{u_{x_i}}(Y) \equiv \left  \frac{\partial f}{\partial x_i} \right  u(x_i)$ [W m <sup>-2</sup> ]
Soil heat flux	$u_c(\bar{\varphi})$	Eq. (36)	n/a	n/a
Natural variation	$u_{NAT}(\bar{\varphi})$	Eq. (26)	n/a	Eq. (26)
Traceable calibration	$u_{CAL}(\bar{\varphi})$	Eq. (27)	n/a	Eq. (27)
FDAS (signal)	$u_{FDAS(TT)}(V_{cur_{MA}})$	Eq. (28)	Eq. (18)	Eq. (30)
FDAS (signal)	$u_{FDAS(TT)}(V_{s_{MAX}})$	Eq. (28)	Eq. (19)	Eq. (31)
In-situ cal. FDAS	$u_c(V_a)$	Eq. (34)	Eq. (20)	Eq. (35)
FDAS (signal)	$u_{FDAS(TT)}(V_s(t_0))$	Eq. (32)	Eq. (12)	Eq. (33)



Title: NEON Algorithm Theoretical Basis Document (ATBD): TIS Soil Heat Flux		Date: 02/05/2020
NEON Doc. #: NEON.DOC.000814	Author: N. Pingintha-Durden	Revision: B

FDAS (signal)	$u_{FDAS(TT)}(V_S(t_{180}))$	Eq. (32)	Eq. (13)	Eq. (33)
FDAS (signal)	$u_{FDAS(TT)}(V_S(t_c))$	Eq. (32)	Eq. (14)	Eq. (33)

## 7 FUTURE PLANS AND MODIFICATIONS

The frequency of self-calibrations (see AD[09]), time period of self-calibrations (see  $t_c$  in Eq.(1)), calibration heater quality flag threshold (see  $d$  in Eq.(7)), and *in-situ* correction flag thresholds (see (see a, b, and c in Eq.(8)) may change to site-specific values.

Future system flags may be incorporated into the data stream and included in the QA/QC summary DP ( $Qsum_{1min}$  and  $Qsum_{30min}$ ) that summarizes any flagged data that went into the computation of the L1 DP.

QA/QC tests may be expanded to include consistency analyses among similar measurement streams. A QA/QC flag for data consistency will be applied according to the redundancy analysis outlined in AD[05], and a pass (flag = 0) or fail (flag = 1) flag will be generated to reflect this analysis. Assume soil type and ground cover are the same among soil plots at a given site and assume that the position of sensors are located within the soil array as shown in Figure 3a. To evaluate soil heat flux for consistency, L1 soil heat flux from a given HFP01SC sensor (a HFP01SC sensor at position 2) will first be compared to the HFP01SC sensor at position 1. If a difference between the two soil heat flux measurements is less than the defined limits (provided by FIU and maintained in the CI data store) then the sensor will have passed its consistency analysis. Alternatively, a soil heat flux difference between the HFP01SC sensors outside the defined limits will result in a failed test. A failed test between the sensors in position 1 and 2, will result in the HFP01SC sensor at position 2 being compared to the sensor at position 3. If this too results in a failed test, then the HFP01SC sensor will have failed the consistency test and be flagged as such (Figure 3b). If the HFP01SC sensor fails the first test but passes the second then it will have passed the consistency test. This test structure helps to ensure that non-functional sensors (e.g. sensors that are faulty or due for service) do not bias the test, since a resulting failed test will allow the sensor to be compared to the other one. Accordingly, the sensors at position 1 and 3 will be first compared to the nearby soil plot (sensor at position 2) and then to each other. L1 DPs that fail the Consistency Analysis will continue to be reported, but will have an associated failed flag that will be include in the QA/QC summary. Note that the evaluation procedures of soil heat flux for consistency may not be applied if soil type and ground cover are not consistent amongst the soil plots.

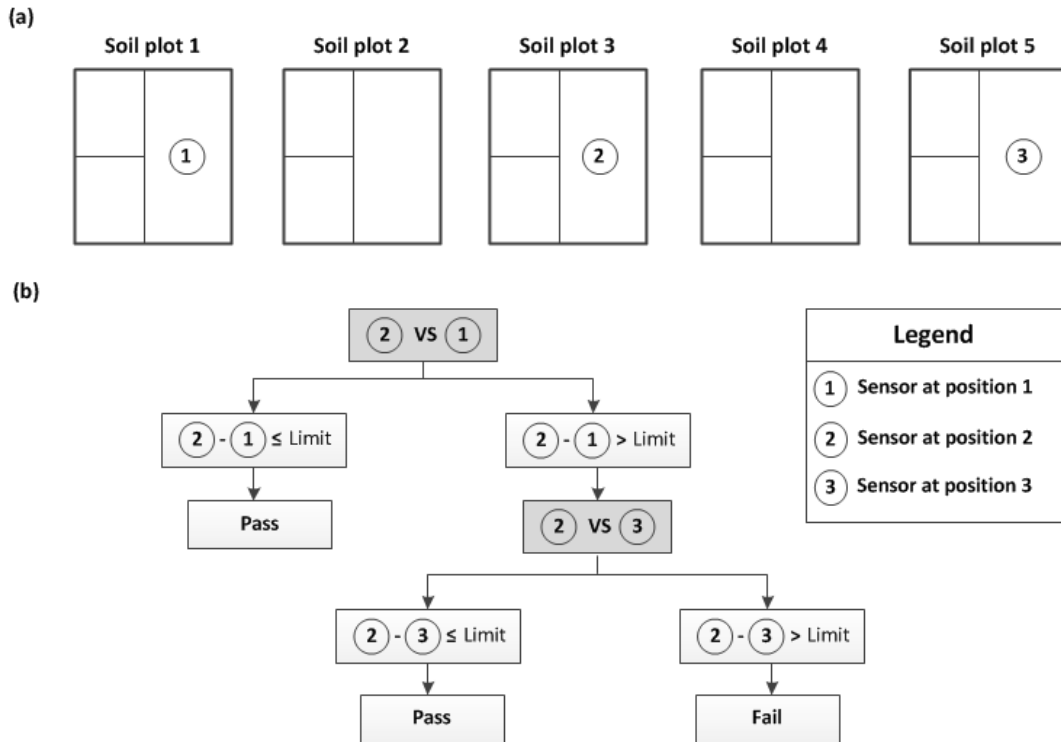


**Figure 3.** (a) Diagram of the position of the HFP01SC sensors within the soil array and (b) consistency test flow diagram for the HFP01SC sensor deployed at position 2.

## 8 BIBLIOGRAPHY

Joint Committee for Guides in Metrology (JCGM) (2008) Evaluation of measurement data – Guide to the expression of uncertainty in measurement. pp. 120.

JCGM (2012) International vocabulary of metrology – Basic and general concepts and associated terms (VIM). 3rd Edition. pp. 92

Ochsner, T.E., Sauer, T.J., and Horton, R. (2006) Field tests of the soil heat flux plate method and some alternatives. *Agronomy Journal*, **98**, 1005-1014.

Ochsner, T.E., Sauer, T.J., and Horton, R. (2007) Soil heat storage measurements in energy balance studies. *Agronomy Journal*, **99**, 311-319.

Sauer, T.J. and Horton, R. (2005) Soil heat flux. In Hatfield, J.L., and J.M. Baker (Eds). *Micrometeorology in Agricultural Systems*, Agronomy Monograph, **47**, pp. 131-154. Madison, Wisconsin, USA.

Taylor, J. R. (1997) An Introduction to Error Analysis: The Study of Uncertainties in Physical Measurements. University Science Books, Mill Valley, California.



**neon**  
Operated by Battelle

<i>Title:</i> NEON Algorithm Theoretical Basis Document (ATBD): TIS Soil Heat Flux		<i>Date:</i> 02/05/2020
<i>NEON Doc. #:</i> NEON.DOC.000814	<i>Author:</i> N. Pingintha-Durden	<i>Revision:</i> B